Neutron fibres: a three-dimensional analysis of bending losses

2000 J. Phys. D: Appl. Phys. 33 1666

(http://iopscience.iop.org/0022-3727/33/14/306)

J. Phys. D: Appl. Phys. **33** (2000) 1666–1673. Printed in the UK PII: S0022-3727(00)02381-0

Neutron fibres: a three-dimensional analysis of bending losses

María L Calvo

Departamento de Optica, Facultad de Ciencias Físicas, Universidad Complutense, 28040, Madrid, Spain

Received 8 March 1999, in final form 20 March 2000

Abstract. The confined propagation of slow neutrons along waveguides of a small cross section (fibres), discussed theoretically some time ago and demonstrated experimentally by other authors later, is analysed further. Motivated by those experiments, a three-dimensional quantum-mechanical treatment of the associated bending losses is presented. An approximate (two-parameter) formula is derived for the transmission coefficient Υ of the curved fibre, which displays its explicit dependence on the curvature radius R_{cu}, for $0 < R_{cu} < +\infty$. By adjusting one of the parameters (b), consistently with the theoretical analysis, and by fitting the other, the approximate formula describes all measured data for Υ. The parameter b (which accounts for the experimental data for Υ at large R_{cu}) allows the estimation of the number of effectively excited modes in the fibre.

1. Introduction

Hollow guides of a suitably large cross section allow for the transport of slow neutron beams along relatively long distances, by multiple internal reflection (see, for instance, Jacrot 1970). Bending losses of the waveguide (associated to radiation due its curvature) stand as one of the main mechanisms responsible for a decrease in the flux transmitted along it. Studies of bending losses in neutron guides of an adequately large cross section can be found, for instance, in Jacrot (1970) and Schaerpf and Eichler (1973). On the other hand, confined propagation of slow (say, thermal) neutrons along waveguides of a small cross section (fibres), and a quantum-mechanical formulation through propagation modes, have been described theoretically (Alvarez-Estrada and Calvo 1984, Calvo and Alvarez-Estrada 1986). The corresponding bending losses in two-dimensional neutron fibres have already been analysed (Calvo and Alvarez-Estrada 1986).

A very important experimental implementation of neutron fibres has been achieved (Kumakhov and Sharov 1992, Chen *et al* 1992). In these works, bundles of polycapillary glass fibres were employed for the confined propagation and focusing of thermal and cold neutrons. Each polycapillary glass fibre contains many hollow capillary channels. A single hollow capillary channel is conceptually analogous to the single neutron fibre discussed theoretically in Alvarez-Estrada and Calvo (1984), and Calvo and Alvarez-Estrada (1986). Such capillary fibres were not straight, and important issues were an experimental determination of the bending losses and an understanding of them (Chen *et al* 1992).

Motivated by these experimental findings, a quantum-mechanical analysis of bending losses in a curved neutron fibre in three spatial dimensions seems in order. It will be the main subject of this present work. We shall also treat the physical features related to the neutron modes and beam propagation. The treatment of bending losses to be presented here will generalize, in a new setting, a previous study about electromagnetic radiation due to curvature in an optical fibre (Calvo and Alvarez-Estrada 1987). This last reference gave various formal details, not to be repeated here, for the similar (but not quite identical) electromagnetic case. This work also provides references to various studies about optical waveguides and their bending losses (see, in particular, Marcuse 1972, 1974, 1976, Snyder and Love 1983 and Marcatili 1969).

Section 2 will discuss some physical features of the devices employed in Kumakhov and Sharov (1992) and Chen *et al* (1992), so as to motivate the present theoretical analysis. Section 3 will summarize essentials about propagation modes for neutrons in thin straight waveguides. Section 4 will deal with curved fibres and the neutron wave function. In section 5, the probability fluxes for the incoming beam and for an emitted one (due to curvature) will be computed. In section 6, an approximate formula for the transmission coefficient of the curved fibre, as a function of the curvature radius R_{cu}, is given and compared to the measured experimental data. Section 7 contains the conclusions and discussions.

2. Physical features

In the experiments described in Kumakhov and Sharov (1992) and Chen *et al* (1992), multicapillary fibres were employed. Any of such polycapillary fibres has, typically, a diameter $d_{pf} = 0.4$ mm and a length between, say, 150 mm and 200 mm and it contains more than $N_{pf} = 1000$

0022-3727/00/141666+08$30.00

individual parallel capillary channels. In turn, each single hollow capillary channel has an internal diameter $d_{\rm hcc}$ = 6 μm and can be regarded as a hollow waveguide of a very small cross section, along which the neutrons propagate. Throughout this work, whenever we refer to a neutron fibre, we shall always deal with one of these individual hollow capillary channels with a small cross section. To avoid confusion, neither a polycapillary fibre nor a bundle thereof (which have much larger cross sections) will be called neutron fibres. The average distance, $d_{\rm nhc}$, between two neighbouring (parallel) hollow capillary channels can be estimated from $d_{\rm pf}^2 \simeq d_{\rm nhc}^2 N_{\rm pf}$. One finds $d_{\rm nhc} \simeq 5$ to 10 μm. The fibres may be straight or bent: in the latter case, they have curvature radius $R_{\rm cu} \geqslant 0.1$ m (metres). Each polycapillary fibre is made of lead–silica glass (Kumakhov and Sharov 1992, Chen *et al* 1992, Kumakhov and Komarov 1990). Accordingly, each of the above hollow capillary channels is surrounded by a lead–silica clad: the latter has a width of about 5 μm, so that, beyond such a distance, the cladding region ends and another neighbouring parallel hollow channel is found.

We suppose that the average energy of one neutron in a typical beam may be about 10^{-2} eV (for thermal neutrons) or about 10^{-4} eV (for cold neutrons), so that the average neutron velocity v is about 10^3 or 10^2 m s^{-1}, respectively. If Φ denotes a typical neutron flux (for instance, $\Phi = 10^{15}$ neutrons cm^{-2} s^{-1}), the average smallest separation between two neighbouring neutrons propagating in the beam is about $d_{\rm n-n} = (v\Phi^{-1})^{1/3}$. For both thermal and cold neutrons, $d_{\rm n-n}$ is of the order of 100 Å. For both thermal and cold neutrons, the beam is not monochromatic so that, in each case, a spectrum of wavelengths is met: for instance, it ranged between 2 Å and 9 Å in the experiments in Chen *et al* (1992). Since these intervals are smaller than $d_{\rm n-n}$, one can reasonably neglect the overlaps between the wave packets associated to different neutrons in the beam and regard each confined neutron as propagating independently.

A priori, one could entertain the possibility that one neutron, propagating initially confined along a certain hollow capillary channel (denoted by hcc1), could escape, by transmission through the surrounding clad due to a quantum-mechanical tunnel effect, to one of the neighbouring parallel hollow capillary channels. Let d be the radial distance from the internal surface limiting the hcc1 to some point in its surrounding clad, so that $0 \leqslant d \leqslant 5$ μm. As estimated in a previous work (Calvo and Alvarez-Estrada 1986), the probability for such a tunnel effect is exponentially small for values of the number of nuclei per cm^3 and of the neutron–nucleus scattering amplitude typical of those in the lead–silica clad, provided that $d \geqslant 0.5$ μm = $d_{\rm tu}$ ($d_{\rm tu}$ being some characteristic tunnel effect length). Consequently, since $d_{\rm nhc}$ is about one order of magnitude larger than $d_{\rm tu}$, one concludes that such a tunnel effect is negligible (absence of 'cross-talk'). Equivalently, one could simply say that neutrons propagate confined along any individual hollow capillary channel as if the latter were surrounded by a clad of infinite width (say, as if $d_{\rm nhc} = \infty$), which will simplify the analysis. This will be the point of view adopted here.

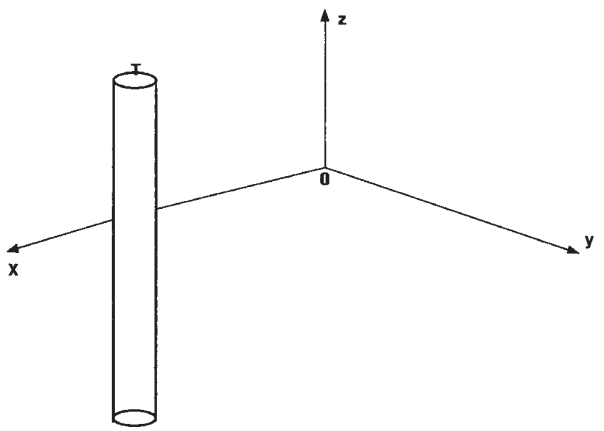

Figure 1. Unbent three-dimensional waveguide (fibre) with a (small) transverse cross section T. In this, and in figures 2 and 3, O represents the origin of coordinates, which lies far from the fibre.

3. Unbent fibre: essentials about propagation modes

Imagine, in three-dimensional space, a straight fibre with infinite length and vanishing curvature, and a finite transverse cross section T, in principle, with arbitrary shape (see figure 1). The z-axis is parallel to (any axis of) the fibre so that T lies in the (x, y)-plane. Three- and two-dimensional vectors will be represented by arrows and boldface symbols, respectively. Thus, the position vector is $\vec{x} = (x, y, z) = (\boldsymbol{x}, z)$. The z-axis and the origin $\vec{x} = (0, 0, 0)$ lie outside the fibre. The confined propagation of neutrons along the fibre can be modelled through the (z-independent) potential $V(\vec{x}) = V(\boldsymbol{x})$: $V(\boldsymbol{x}) = V_{\rm c} = 2\pi\hbar^2 b_{\rm c}\rho_{\rm c}/m_{\rm n}$ if $\boldsymbol{x}$ lies inside the inner part of T (the core, represented by the subscript c), while $V(\boldsymbol{x}) = V_{\rm cl} = 2\pi\hbar^2 b_{\rm cl}\rho_{\rm cl}/m_{\rm n}$ for $\boldsymbol{x}$ outside T (the infinite outer medium or clad, with subscript cl). Here, $\hbar$ denotes Planck's constant, $m_{\rm n}$ is the neutron mass, $b_{\rm i}$ is the average coherent amplitude for the low-energy scattering of a neutron by an atomic nucleus belonging to i=c or cl and $\rho_{\rm i}$ is the number of nuclei per cm^3 in them. For confined neutron propagation along the fibre to occur, it is necessary that $V_{\rm c} < V_{\rm cl}$.

We shall deal with a neutron beam (coming, say, from a nuclear reactor), which, in general, has an energy spectrum and propagates confined along the fibre, with constant flux (at least, in some average sense). Let any neutron in the beam be described by a time(t)-dependent wave function $\psi(\vec{x}; t)_{\rm in}$, which is a linear superposition of stationary wave functions $\psi(\vec{x}; E)_{\rm in} \exp(-{\rm i}Et/\hbar)$, where $E(> V_{\rm cl})$ is the total neutron energy. $\psi(\vec{x}; E)_{\rm in}$ satisfies, for any $\vec{x}$ inside or outside the fibre, the time-independent Schrödinger equation:

$$\left[-\frac{\hbar^2}{2m_{\rm n}}\left[\Delta_T + \frac{\partial^2}{\partial z^2}\right] + V(\vec{x})\right]\psi(\vec{x}; E)_{\rm in} = E\psi(\vec{x}; E)_{\rm in} \tag{1}$$

where $\Delta_T = \partial^2/\partial x^2 + \partial^2/\partial y^2$. Physically, $\psi(\vec{x}; E)_{\rm in}$ should be chosen to be a propagation mode $\phi(\boldsymbol{x})_\alpha \exp({\rm i}\beta_\alpha z)$ with propagation constant β_α (Re $\beta_\alpha > 0$, Re denoting the real part). Since there is an energy spectrum

($V_{\rm cl} < E_{\rm min} \leqslant E \leqslant E_{\rm max}$), one has, for any $\boldsymbol{x}$:

$$\psi(\vec{x};t)_{\rm in} = \sum_{\alpha} \int_{E_{\rm min}}^{E_{\rm max}} {\rm d}E c(E)_\alpha \phi(\boldsymbol{x})_\alpha \times \exp({\rm i}\beta_\alpha z)\exp(-{\rm i}Et/\hbar) \quad (2)$$

where $c(E)_\alpha$ is a given amplitude, characterizing that incoming beam. The description through equation (2) will be revised later. α denotes a set of additional quantum numbers, also required in order to specify uniquely (together with either E or β_α) the propagation mode. Equation (1) yields:

$$\left[-\frac{\hbar^2}{2m_{\rm n}}\Delta_T + V(\boldsymbol{x}) - V_{\rm cl}\right]\phi(\boldsymbol{x})_\alpha = -\frac{\hbar^2}{2m_{\rm n}}\chi_\alpha^2\phi(\boldsymbol{x})_\alpha \quad (3)$$

$$E = V_{\rm cl} + \frac{\hbar^2}{2m_{\rm n}}\beta_\alpha^2 - \frac{\hbar^2}{2m_{\rm n}}\chi_\alpha^2. \quad (4)$$

Notice that ${\rm Re}\,\chi_\alpha > 0$. If both $b_{\rm cl}$ and $b_{\rm c}$ are real, then so are β_α and χ_α: this will be the case for a hollow fibre with negligible absorption of neutrons by the clad, to be assumed in this work. There is a finite set of real negative eigenvalues $-\chi_\alpha^2$ of equation (3), fully determined by this equation. Then, for given E, there is only a finite set of values of β_α determined by equation (4) (for the finite set of allowed values of χ_α^2). $\phi(\boldsymbol{x})_\alpha$ are normalized so that:

$$\int {\rm d}^2\boldsymbol{x}\phi(\boldsymbol{x})_\alpha^{(*)}\phi(\boldsymbol{x})_{\alpha'} = \delta_{\alpha,\alpha'} \quad (5)$$

where $\delta_{\alpha,\alpha'}$ denotes a Kronecker delta and the integration is carried out over the whole infinite $\boldsymbol{x}$-plane. Upon integrating in equation (5), equation (3) implies:

$$\chi_\alpha^2\int {\rm d}^2\boldsymbol{x}\,|\phi(\boldsymbol{x})_\alpha|^2 + \left[-\int {\rm d}^2\boldsymbol{x}\phi(\boldsymbol{x})_\alpha^{(*)}\Delta_T\phi(\boldsymbol{x})_\alpha\right] = \frac{2m_{\rm n}}{\hbar^2}\int {\rm d}^2\boldsymbol{x}\,[-V(\boldsymbol{x}) + V_{\rm cl}]\,|\phi(\boldsymbol{x})_\alpha|^2\,.$$

The second integral in the left-hand-side of the last equation is never negative (as an integration by parts shows) and $V(\boldsymbol{x}) - V_{\rm cl} = 0$ if $\boldsymbol{x}$ lies outside T. Then, using equation (5), one gets readily the useful bound:

$$\chi_\alpha \leqslant [4\pi(b_{\rm cl}\rho_{\rm cl} - b_{\rm c}\rho_{\rm c})]^{1/2} \equiv \chi_{\rm max}. \quad (6)$$

The fundamental mode corresponds to the largest possible value of $\chi_\alpha(>0)$ compatible with the bound in equation (6). As one proceeds to higher modes, the associated values of $\chi_\alpha(>0)$ decrease in magnitude.

The total number of allowed propagation modes in the actual unbent fibre, namely, the total number of independent solutions of equation (3) as α varies, can be estimated, in quasi-classical approximation, as: $N_{\rm pm} = 2A(T)(b_{\rm cl}\rho_{\rm cl} - b_{\rm c}\rho_{\rm c})$, where $A(T)$ is the area of T. Similarly, the number of propagation modes having χ_α^2 in the range $0 \leqslant \chi_0^2 \leqslant \chi_\alpha^2 \leqslant \chi_{\rm max}^2$ is estimated to be (also in quasi-classical approximation) $N_{\rm pm}(\chi_0^2) = (2\pi)^{-1}A(T)\chi_0^2$. Then, the fraction of propagation modes with $0 \leqslant \chi_0^2 \leqslant \chi_\alpha^2 \leqslant \chi_{\rm max}^2$ over the total number of them is $\chi_0^2/\chi_{\rm max}^2$ (Martin 1972, Berry and Mount 1972, Calvo and Alvarez-Estrada 1986). It is not warranted, *a priori*, that all allowed propagation modes will be effectively excited. Neutrons, as they enter into the hollow capillary channel, may find a greater difficulty to propagate into a mode, the smaller χ_α is for the latter. An estimate of the number of propagation modes which do get excited effectively stands as an interesting open problem. The set of quantum numbers α over which the summation in equation (2) runs, corresponds to all modes which effectively propagate.

For the actual hollow capillary channel ($b_{\rm c}\rho_{\rm c} = 0$) and values of the number of nuclei per cm^3 and of the neutron–nucleus scattering amplitude $b_{\rm cl}$ (>0) (Bacon 1962), typical of those in the clad, one expects that the right-hand side of equation (6) ranges from about 10^{-3} Å to about 10^{-2} Å. Then, for typical values of β_α ranging from, say, 0.7 Å^{-1} to 3 Å^{-1}, χ_α/β_α for the highest modes (say, the fundamental one and the first few above it) varies from 10^{-2} to 10^{-4}. On the other hand, $N_{\rm pm}$ varies between 4.5×10^2 and 4.5×10^4.

In spite of the relatively large number of allowed propagation modes, and even if the inner diameter of a hollow capillary channel ($d_{\rm hcc} = 6$ μm) is about three orders of magnitudes larger than the average de Broglie wavelength of a neutron, a quantum-mechanical description for neutrons propagating confined (after having entered into the fibre from outside) should be allowed as another possible approach in principle, instead of disregarding it from the outset, as if it were an academic undertaking. Thus, for certain effectively propagating modes (namely, the fundamental one and a subset of higher modes above it), $\chi_\alpha(d_{\rm hcc}/2)$ may be of order unity and even larger and, hence, quantum effects may be important. In fact, for values typical of the actual hollow capillary channel, equation (6) implies that $\chi_\alpha d_{\rm hcc}$ has an upper bound which varies between 2.8 and 28.

The reliability of the quantum mechanical description will also be justified *a posteriori*, since it will allow the treatment of bending losses through a method different from the geometrical optics one presented by Kumakhov and Komarov (1990). In particular, it will lead to an estimate of the number of effectively propagating modes.

4. Curved fibre: asymptotic wave function

From now on, it will be supposed that the infinite three-dimensional fibre is perfectly straight from $z = -\infty$ up to some finite $z = z_0$ and that it has a large curvature radius $R_{\rm cu}$ for $z_0 < z < +\infty$ (see figure 2). $R_{\rm cu}$ will always be much larger than any neutron wavelength and larger than $d_{\rm hcc}$, say, $R_{\rm cu} \geqslant 0.1$ m (compared with in section 6). For those values of $R_{\rm cu}$ (which we shall qualify as 'large'), all mathematical operations to be performed will be valid. For convenience, the whole fibre is taken to lie far from the origin $\vec{x} = (0,0,0)$. Let an incoming neutron propagate confined along the fibre from $z = -\infty$ towards $z = z_0$, so that it is represented by the propagation mode $\phi(\boldsymbol{x})_\alpha\exp({\rm i}\beta_\alpha z)$, which fulfils the various conditions treated in section 3. For $z > z_0$, where the thin waveguide is curved, there will be a finite probability (actually, increasing, as z increases) for the neutron to escape towards the infinite clad. The propagation of the neutron for any $\vec{x}$, as determined by that incoming $\phi(\boldsymbol{x})_\alpha\exp({\rm i}\beta_\alpha z)$, is described by a (time-independent) wave function $\psi(\vec{x})_\alpha$, which also fulfils equation (1). The latter can be transformed, through standard techniques, into the

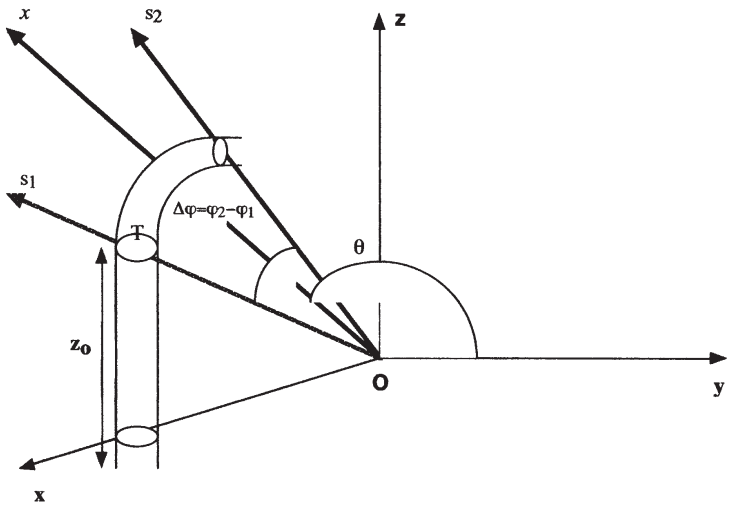

Figure 2. Definition of angles and reference axes in the bent three-dimensional fibre: z_0, the unbent part of the fibre ($z_0 > 0$). The part of the fibre above z_0 is curved. The axes, Os_1 and Os_2, which lie in the (x, z)-plane, form the angles φ_1 and φ_2, respectively, with the x-axis. $\Delta\varphi = \varphi_2 - \varphi_1$ is the angle defining the bent region, between the axes Os_1 and Os_2. θ is the angle between the y-axis and the vector $\vec{x}$. The radius of the curvature R_{cu} is the distance from the origin O up to the centre of the (small) cross section T of the fibre.

following homogeneous integral equation:

$$\psi(\vec{x})_\alpha = -\frac{2m_n}{\hbar^2}\int \mathrm{d}^3\vec{x}' G(\vec{x}-\vec{x}')\left[V(\vec{x}') - V_{cl}\right]\psi(\vec{x}')_\alpha. \tag{7}$$

The integration is extended over the whole region occupied by the fibre, where $V(\vec{x}') - V_{cl}$ is non-vanishing. G is the standard three-dimensional Green's function, namely: $[\Delta_T + \partial^2/\partial z^2 + k^2]G(\vec{x}-\vec{x}') = -\delta^3(\vec{x}-\vec{x}')$, with $k^2 = 2m_n\hbar^{-2}(E - V_{cl})$ ($\delta^3(\vec{x}-\vec{x}')$ being Dirac's delta function). One has:

$$G(\vec{x}-\vec{x}') = \frac{1}{4\pi}\frac{\exp \mathrm{i}k|\vec{x}-\vec{x}'|}{|\vec{x}-\vec{x}'|}. \tag{8}$$

Using the above properties of $G(\vec{x}-\vec{x}')$, it is easy to prove that the right-hand side of equation (7) fulfils equation (1) (see, for example, Glauber 1959 and Sears 1989). We accept that no inhomogeneous term (say, neither $\phi(\boldsymbol{x})_\alpha \exp(\mathrm{i}\beta_\alpha z)$ nor any plane wave) should appear in the right-hand side of equation (7), contrary to what happens in standard scattering problems. This fact appears to be consistent with the incoming boundary condition, namely, the reduction of $\psi(\vec{x})_\alpha$ to $\phi(\boldsymbol{x})_\alpha \exp(\mathrm{i}\beta_\alpha z)$ at $z = -\infty$, which always 'sees' the action of $V(\vec{x})$. The applications of this recipe to other two- and three-dimensional cases (Calvo and Alvarez-Estrada 1986, 1987) have led to consistent results. It is useful to introduce spherical coordinates with respect to $\vec{x} = (0, 0, 0)$ and to the y-axis (instead of the z-axis), so that $\vec{x} = |\vec{x}|(\cos\varphi\sin\theta, \cos\theta, \sin\varphi\sin\theta)$. Let $|\vec{x}|$, φ and θ be fixed, so that $|\vec{x}| \gg R_{cu}$, φ is arbitrary and θ is close to $\pi/2$. Then, one has the following result:

$$\psi(\vec{x})_\alpha \simeq \frac{R_{cu}}{|\vec{x}|}\exp \mathrm{i}\left[k|\vec{x}| + R_{cu}\beta_\alpha(\varphi + 2^{-1}\pi)\right] \times \frac{\exp \beta_\alpha R_{cu}\Lambda_\alpha(\theta)}{2[2\pi R_{cu}\gamma_{1,\alpha}(\theta)]^{1/2}} B_\alpha(\theta). \tag{9}$$

In equation (9):

$$B_\alpha(\theta) = -\frac{2m_n}{\hbar^2}\int \mathrm{d}^2\boldsymbol{x}'\left[V(\boldsymbol{x}') - V_{cl}\right]\phi(\boldsymbol{x}')_\alpha \exp y'\gamma_{1,\alpha}(\theta) \tag{10}$$

$$\Lambda_\alpha(\theta) = \frac{\gamma_{1,\alpha}(\theta)}{\beta_\alpha} - \frac{1}{2}\ln\left[\frac{1 + (\gamma_{1,\alpha}(\theta)/\beta_\alpha)}{1 - (\gamma_{1,\alpha}(\theta)/\beta_\alpha)}\right] \tag{11}$$

$$\gamma_{1,\alpha}(\theta) = \left[\beta_\alpha^2 - \hbar^{-2}2m_n(E - V_{cl})\sin^2\theta\right]^{1/2} \tag{12}$$

where ($\boldsymbol{x}' = (x', y')$). The proof of equations (9) and (10) is similar to the one presented for optical waveguides in Calvo and Alvarez-Estrada (1987), to which we refer for details and comparisons with other related (but not identical) approximations by other authors. Since $E - V_{cl} > 0$ (say, $\beta_\alpha > \chi_\alpha$: see equation (4)), one sees that $\gamma_{1,\alpha}(\theta) \geqslant \chi_\alpha > 0$ and that $1 \geqslant \gamma_{1,\alpha}(\theta)/\beta_\alpha$. Upon expanding into a power series in $\gamma_{1,\alpha}(\theta)/\beta_\alpha$, one sees that $\Lambda_\alpha(\theta) < 0$ holds.

Let the incoming neutron, propagating confined along the fibre from $z = -\infty$ towards $z = z_0$, be represented by the linear superposition given in equation (2). Consequently, the propagation of the neutron for any $\vec{x}$ (in particular, for $z > z_0$, outside the fibre) is described by:

$$\psi(\vec{x}; t) = \sum_\alpha \int_{E_{min}}^{E_{max}} \mathrm{d}E c(E)_\alpha \psi(\vec{x})_\alpha \exp(-\mathrm{i}Et/\hbar) \tag{13}$$

where $\psi(\vec{x})_\alpha$ is the solution of equation (7). Then, equations (13) and (9) characterize the behaviour of the neutron wave function for any fixed $|\vec{x}|$, φ and θ, such that $|\vec{x}| \gg R_{cu}$, φ is arbitrary and θ is close to $\pi/2$.

5. Probability fluxes

The quantum-mechanical probability current determined by a wave function $\Psi(\vec{x}; t)$ (like those in equations (2) or (13)), is

$$\vec{J}(\vec{x}; t) = \frac{\hbar}{m_n}\mathrm{Re}\left[\Psi(\vec{x}; t)^*(-\mathrm{i}\vec{\nabla})\Psi(\vec{x}; t)\right]. \tag{14}$$

First, we shall treat the quantum-mechanical probability flux $F_{\rm in}$ of the incoming wave given in equation (2) across the whole (x, y)-plane, for any z in $-\infty < z < z_0$. Equation (14) (with $\Psi(\vec{x};t) = \psi(\vec{x};t)_{\rm in}$) and equation (5) yield:

$$F_{\rm in} = m_{\rm n}^{-1}\hbar \sum_{\alpha} \int_{E_{\rm min}}^{E_{\rm max}} {\rm d}E \int_{E_{\rm min}}^{E_{\rm max}} {\rm d}E' \beta_\alpha(E) \times c(E)_\alpha \beta_\alpha(E') c(E')^*_\alpha \exp\left[{\rm i}(E'-E)t/\hbar\right] \quad (15)$$

which is not constant, but time-dependent. In order to have neutron fluxes which are both non-monochromatic and constant (at least, in some average sense), we shall describe any neutron by statistical mixtures (Messiah 1961) of wave functions $\Psi(\vec{x};t)$ like those in equations (2) and (13). Here, such statistical mixtures will be characterized by statistical averages ($\langle\ \rangle$) of physical quantities bilinear in $\Psi(\vec{x};t)$ and $\Psi(\vec{x};t)^*$, to be evaluated using

$$\langle c(E)_\alpha c(E')^*_{\alpha'}\rangle = \delta(E-E')e(E)_{\alpha,\alpha'} \quad (16)$$

where $\delta(E-E')$ denotes Dirac delta functions and $e(E)_{\alpha,\alpha'}$ is some spectral density, characterizing the beam. Probability fluxes will be understood and evaluated as statistical averages. This statistical description agrees conceptually with typical averaging procedures over the source energy spectrum and with other descriptions (say, Maxwellian distributions), previously employed for free thermal neutrons produced in nuclear reactors (see, for instance, Schaerpf and Eichler 1973). That description of a neutron also plays a role entirely analogous to that of partially coherent light (compare with Born and Wolf 1999). Then, equations (15) and (16) yield the incoming probability flux as:

$$\langle F_{\rm in}\rangle = \frac{\hbar}{m_{\rm n}} \sum_{\alpha} \int_{E_{\rm min}}^{E_{\rm max}} {\rm d}E \beta_\alpha e(E)_{\alpha,\alpha}. \quad (17)$$

Next, we shall evaluate $\langle \vec{J}(\vec{x};t)\rangle = \langle \vec{j}(\vec{x})\rangle$ when $\Psi(\vec{x};t)$ is given in equation (13), for $|\vec{x}| \gg R_{\rm cu}$, arbitrary φ and θ close to $\pi/2$. Upon expressing $\vec{\nabla}$ in spherical coordinates and retaining only the leading contribution, one finds:

$$\langle \vec{j}(\vec{x})\rangle \simeq \frac{\vec{x}}{|\vec{x}|}\left|\langle \vec{j}(\vec{x})\rangle\right| \quad (18)$$

$$\left|\langle \vec{j}(\vec{x})\rangle\right| = \frac{R_{\rm cu}}{|\vec{x}|^2} \sum_{\alpha,\alpha'} \int_{E_{\rm min}}^{E_{\rm max}} {\rm d}E \times \exp\left[R_{\rm cu}(\beta_\alpha \Lambda_\alpha(\theta) + \beta_{\alpha'}\Lambda_{\alpha'}(\theta))\right] D_{\alpha,\alpha'}(\theta) \quad (19)$$

$$D_{\alpha,\alpha'}(\theta) = \frac{k\hbar}{8\pi m_{\rm n}} \frac{{\rm Re}[e(E)_{\alpha,\alpha'} B_{\alpha'}(\theta)^{(*)} B_\alpha(\theta)]}{[\gamma_{1,\alpha}(\theta)\gamma_{1,\alpha'}(\theta)]^{1/2}} \quad (20)$$

where $\langle \vec{j}(\vec{x})\rangle$ is essentially concentrated in the following solid angle Ω about $(\cos\varphi, 0, \sin\varphi)$. Ω is determined by the angles $\pi/2-\theta_0 < \theta < \pi/2+\theta_0$ and $\varphi_1 < \varphi < \varphi_2$, where θ_0 is small. φ_1 and φ_2 are, respectively, the values of φ at which the fibre starts to bend (which corresponds to $z = z_0$) and terminates—a large value of z, as $R_{\rm cu}$ is large compared to $d_{\rm hcc}$ (see figure 2). We shall evaluate the probability flux ($\langle F_{\rm loss}\rangle$) of $\langle \vec{j}(\vec{x})\rangle$ across the finite surface Σ, determined by the intersection of the spherical surface of large radius $|\vec{x}| \gg R_{\rm cu}$ and centre at $\vec{x} = (0,0,0)$ and the solid angle Ω. $\langle F_{\rm loss}\rangle$, which describes how the neutron could escape far outside the curved fibre, reads (${\rm d}\Omega = \sin\theta {\rm d}\theta {\rm d}\varphi$):

$$\langle F_{\rm loss}\rangle = |\vec{x}|^2 \int {\rm d}\Omega \frac{\vec{x}}{|\vec{x}|}\langle \vec{j}(\vec{x})\rangle \simeq |\vec{x}|^2 \tilde{C} \int_{\varphi_1}^{\varphi_2} {\rm d}\varphi \quad (21)$$

$$\tilde{C} = \int_{\pi/2-\theta_0}^{\pi/2+\theta_0} {\rm d}\theta \sin\theta \left|\langle \vec{j}(\vec{x})\rangle\right|. \quad (22)$$

The integral over ${\rm d}\Omega$ in equation (21) has been extended over the solid angle Ω. Notice that $|\langle \vec{j}(\vec{x})\rangle|$ in equation (19) is independent of φ and so is $\tilde{C}$. The probability flux lost per unit length of the curved fibre is $\langle F_{\rm loss}\rangle/[R_{\rm cu}(\varphi_2-\varphi_1)]$. The average bending loss coefficient (with dimension (length)$^{-1}$) is:

$$\tau_{\rm av} = \frac{\langle F_{\rm loss}\rangle}{R_{\rm cu}(\varphi_2-\varphi_1)\langle F_{\rm in}\rangle} = \frac{|\vec{x}|^2\tilde{C}}{R_{\rm cu}\langle F_{\rm in}\rangle}. \quad (23)$$

We shall give the leading contribution to $\tau_{\rm av}$ for suitably large $R_{\rm cu}$. Details of the computation appear in the appendix. One finds (with $\gamma_{1,\alpha}(\pi/2) = \chi_\alpha$):

$$\tau_{\rm av} \simeq \frac{1}{R_{\rm cu}^{1/2} F_{\rm in}} \sum_{\alpha,\alpha'} \int_{E_{\rm min}}^{E_{\rm max}} {\rm d}E \times \exp\left[R_{\rm cu}(\beta_\alpha\Lambda_\alpha(\pi/2) + \beta_{\alpha'}\Lambda_{\alpha'}(\pi/2))\right] \times \frac{\pi^{1/2}}{[\gamma_{1,\alpha}(\pi/2)+\gamma_{1,\alpha'}(\pi/2)]^{1/2}} D_{\alpha,\alpha'}(\pi/2). \quad (24)$$

We now consider the transverse cross section of the fibre at z and let $\langle F(z)\rangle$ be the probability flux of $\langle \vec{j}(\vec{x})\rangle$ across that cross section (see the appendix and figure 3). One has $\langle F(z_0)\rangle \simeq \langle F_{\rm in}\rangle$. As shown also in the appendix, one gets the approximate formula for $z \geqslant z_0$:

$$\langle F(z)\rangle \simeq \langle F_{\rm in}\rangle \exp[-\tau_{\rm av}(z-z_0)]. \quad (25)$$

Equation (25) describes the decrease of the probability flux of the confined neutron propagating along the curved fibre, due to curvature, and it also justifies the physical meaning of $\tau_{\rm av}$. As the curved fibre is not infinite but it ends at some (finite, but large) $z_1 > z_0$, so that $z_1 - z_0 = l$ can be regarded as its length, then $\Upsilon = \langle F(z)\rangle/\langle F_{\rm in}\rangle \simeq \exp[-\tau_{\rm av} l]$ can be interpreted as its transmission coefficient.

The case with N (more or less) parallel hollow capillary channels (with $N \gg 1$), which occurs in reality with the polycapillary fibre (so that $N = N_{\rm pf}$) and with bundles thereof, can be treated similarly, and leads, approximately, to the same $\tau_{\rm av}$ and Υ. In fact: (i) the incoming flux can be taken as $N\langle F_{\rm in}\rangle$ and the radiated probability flux due to bending can be approximated as $N\langle F_{\rm loss}\rangle$ (upon neglecting, as a first approximation, the possibility that the probability radiated by one hollow capillary channel could be trapped by another one and, then, propagate confined along the second hollow capillary channel); (ii) equation (25) is also multiplied by N.

6. The transmission coefficient of the curved fibre as a function of $R_{\rm cu}$

6.1. An approximate two-parameter formula for Υ

We shall study how $\tau_{\rm av}$ and Υ vary with $R_{\rm cu}$. Notice that $\Lambda_\alpha(\pi/2) = (\chi_\alpha/\beta_\alpha) - 2^{-1}\ln[(1+(\chi_\alpha/\beta_\alpha))(1-(\chi_\alpha/\beta_\alpha))^{-1}]$.

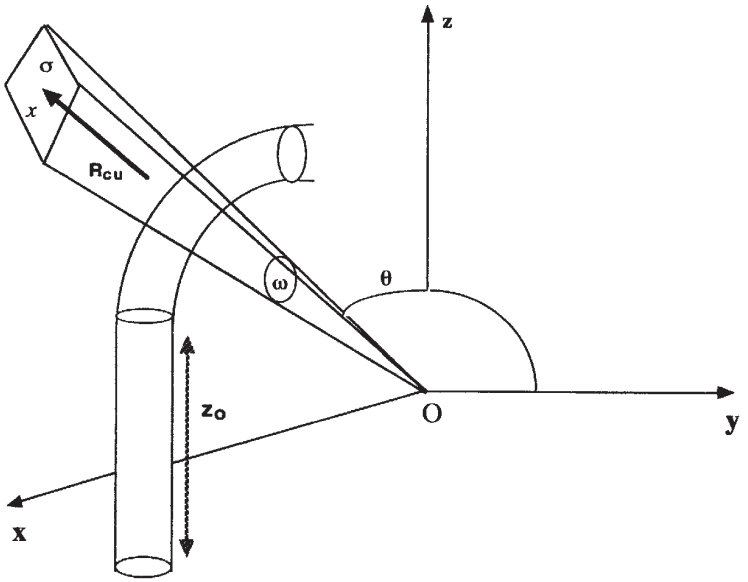

Figure 3. The infinitesimal solid angle ω and the surface σ are displayed. The solid angle ω is limited laterally by the surface $\sigma(\omega)$. The surface, in turn, is formed by four (triangle-like) surfaces $\sigma(\omega; 1)$, $\sigma(\omega; 2)$, $\sigma(\omega; 3)$ and $\sigma(\omega; 4)$. Notice that neither $\sigma(\omega)$ nor $\sigma(\omega; i)$, $i = 1, 2, 3, 4$, are displayed for simplicity. The vector $\vec{x}$ starts at O and ends at the surface σ ($|\vec{x}| \gg R_{cu}$).

For values $\chi_\alpha/\beta_\alpha \leqslant 10^{-2}$ (which always holds in the cases studied in this work), one can approximate $\Lambda_\alpha(\pi/2) \simeq -3^{-1}[\chi_\alpha/\beta_\alpha]^3$.

As R_{cu} becomes very large, the behaviour of τ_{av} is dominated by $\exp[-bR_{cu}]$, b being the minimum of $(2/3)\beta_\alpha[\chi_\alpha/\beta_\alpha]^3 (> 0)$ as β_α and χ_α vary (for the minimum, one sets $\alpha = \alpha'$). Recall that β_α is determined by equation (4) in terms of χ_α (which takes on a finite set of values, determined by equation (3)) and of E (which varies in $V_{cl} < E_{min} < E < E_{max}$). Then, the minimum b is met when $E = E_{max}$ and $\chi_\alpha \equiv \chi_0$ are the smallest in the set of all χ_α which are excited effectively in the unbent part of the fibre: hence, the corresponding $\beta_\alpha \equiv \beta_0$ is the maximum. Thus, we expect that all modes such that $\chi_0 \leqslant \chi_\alpha \leqslant \chi_{max}$ do get excited effectively. Upon recalling section 3, the number of modes which propagate effectively is $N_{pm}(\chi_0^2) = (2\pi)^{-1}A(T)\chi_0^2$ and the fraction of such modes over the total number of them is χ_0^2/χ_{max}^2.

There is some $R_{cu} = R_{cu,0}$ such that, for $R_{cu} < R_{cu,0}$, the factors $\exp[R_{cu}(\beta_\alpha\Lambda_\alpha(\pi/2) + \beta_{\alpha'}\Lambda_{\alpha'}(\pi/2))]$ cease to determine the behaviour of τ_{av}, since the values of $B_{\alpha'}(\theta)^{(*)}B_\alpha(\pi/2)$—and those for the other factors—become more important, for any effectively excited mode α (see the appendix). Then, for $R_{cu} < R_{cu,0}$, the behaviour of τ_{av} is determined by the overall factor $R_{cu}^{-1/2}$.

From the above analysis, it may be reasonable to approximate τ_{av} by the following formula containing two parameters, a and b:

$$\tau_{av} \simeq \frac{a\exp[-bR_{cu}]}{R_{cu}^{1/2}}. \tag{26}$$

The parameter $b = (2/3)\beta_0[\chi_0/\beta_0]^3$ (>0) governs the behaviour of τ_{av} for very large R_{cu}. It is not so easy to give an equally precise formula for a. The latter describes the overall influence of the fraction in the right-hand side of equation (24) ($\times R_{cu}^{1/2}$) in $R_{cu} \leqslant R_{cu,0}$: the summations over α, α' and the integration over E are extended over some set or subset of effectively propagating modes, which is not easy to specify in a more precise way. In spite of this, the overall parameterization in terms of a seems physically meaningful. Thus, we arrive at the announced approximate formula displaying how Υ depends on R_{cu}:

$$\Upsilon \simeq \exp[-al\exp[-bR_{cu}]/R_{cu}^{1/2}]. \tag{27}$$

Let R_{cu} become very large. Then, Υ tends quickly towards unity. As R_{cu} tends to zero, Υ goes quickly to zero.

6.2. Application of the approximate formula to the measured data

The behaviour in equation (27), as R_{cu} varies, appears to be consistent with the data in Chen *et al* (1992) for a suitable adjustment of b and a fit of al. More specifically, equation (27) with either $al \simeq 0.95$ m$^{1/2}$ and $b \simeq 0.51$ m^{-1} or $al \simeq 1$ m$^{1/2}$ and $b \simeq 0.55$ m^{-1} is approximately consistent with figure 3 in Chen *et al* (1992) for, say, 0.1 m $< R_{cu} <$ 13 m. Figure 4 displays our plot for one of those choices of parameters. The value of b has not been predicted, but its order of magnitude seems physically reasonable and essentially consistent with the arguments in the previous subsection (and with estimates of $(2/3)\beta_\alpha[\chi_\alpha/\beta_\alpha]^3$), for typical average values of β_α about 1 Å^{-1} and of χ_α/β_α between 10^{-3} and 10^{-4}). For $b \simeq 0.51$ m^{-1} and a maximum propagation constant for the effectively propagating modes (namely, β_0) about 3 Å^{-1}, one gets $\chi_0/\beta_0 \simeq 2.9 \times 10^{-4}$. The total number of effectively excited modes is, then, estimated to be: $N_{pm}(\chi_0^2) \simeq 340$.

As the right-hand side of equation (6) ranges from about 10^{-3} Å to about 10^{-2} Å, so that N_{pm} varies between 4.5×10^2 and 4.5×10^4, one finds that the ratio $N_{pm}(\chi_0^2)/N_{pm}$ varies

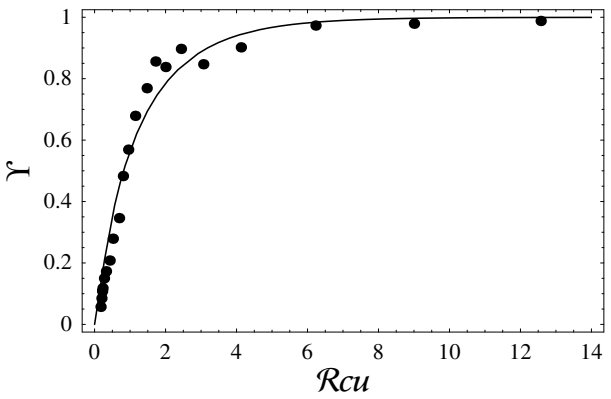

Figure 4. Plot of Υ (equation (27)) as a function of R_{cu} (in metres), for $al \simeq 0.95\ \mathrm{m}^{1/2}$ and $b \simeq 0.51\ \mathrm{m}^{-1}$. For comparison and in order to show the approximate consistency of the former, the experimental data (for a 167 mm fibre) taken from figure 3 in Chen *et al* (1992) are also displayed (the point corresponding to $8.5\ \mathrm{m} < R_{\mathrm{cu}} < 9\ \mathrm{m}$ is a reasonable interpolation of their data).

from 0.8 to 8×10^{-3}. The behaviour of the data in figure 3 in Chen *et al* (1992) changes at $R_{\mathrm{cu},0} \simeq 3$ m. From the analysis in the appendix, we use, in a semi-quantitative sense, $R_{\mathrm{cu},0} \simeq (3\lambda_\alpha/2)(\beta_\alpha/\chi_\alpha)^2 d_{\mathrm{hcc}} \simeq 3$ m with $\lambda_\alpha < 1$ (but not too small), for some average α. Then, one estimates $\chi_\alpha/\beta_\alpha \simeq 10^{-3}$, which is essentially consistent with the above results.

A better assessment of a would require not only further information about $e(E)_{\alpha,\alpha'}$, but also about the effectively excited modes and a more refined evaluation of $B_\alpha(\pi/2)$ and, so, it lies outside the scope of this work. We have not tried to get either the best fit or to set proper errors for the approximate values of al and b. Neither have we tried to assess the sensitivity of our approximate fits to slight variations of l since, as Chen *et al* (1992) remark, their data do not display variations as they increase the length of fibre l from 167 mm to 200 mm.

7. Conclusions

The motivation for this work has been triggered by the experiments, previously cited, in which slow neutrons have been guided along thin waveguides (hollow capillary channels). The quantum-mechanical treatment of the confined neutron propagation, proposed earlier, has been justified further and extended so as to provide a three-dimensional analysis of curvature losses.

The neutron is represented, in general, by a statistical mixture of wave functions, so as to describe a non-monochromatic beam with constant total flux. Then, our definition of the average bending loss coefficient τ_{av} is more general than the ones employed in Snyder and Love (1983), or Calvo and Alvarez-Estrada (1987), since all those authors restricted to only one propagation mode. The behaviour of our τ_{av}, as the curvature radius R_{cu} varies, is fully consistent with that for the analogous coefficient for a bent optical fibre when only one propagation mode is considered (compared, for instance, with Snyder and Love 1983, Calvo and Alvarez-Estrada 1987). For other related studies, also for optical fibres, see Marcuse (1972, 1976) and references therein. If the neutron would have, approximately, a definite energy E (instead of an energy spectrum, still with constant flux), then, all our results are also valid, provided that one omits $\int_{E_{\mathrm{min}}}^{E_{\mathrm{max}}} \mathrm{d}E$, and replaces $e(E)_{\alpha,\alpha'}$ by $c(E)_\alpha c(E)^*_{\alpha'}$.

We stress that the quantum-mechanical formulation has yielded an approximate explicit formula for the transmission coefficient Υ of the curved fibre as a function of R_{cu}, for $0 < R_{\mathrm{cu}} < +\infty$ and, thus, it provides an alternative to the geometric optics treatment employed in Chen *et al* (1992).

The approximate formula for Υ, with some adequate adjustment for the parameter b (consistent with the theoretical analysis) and a fit of the other parameter, is consistent with the measured experimental data.

The behaviour of Υ at large R_{cu} allows to estimate (through b) the number of effectively propagating modes. Such a number is not small, but it is less than the total number of allowed modes.

Acknowledgments

The author is grateful to Dr W M Gibson (Center for X-ray Optics, State University of New York at Albany) for an interesting correspondence and comments regarding guided neutron beams, capillary optics and neutron fibres, and to Mr Gabriel F Calvo for some computational help when fitting the data. The constructive criticisms of the (anonymous) referees are acknowledged. This work is dedicated to the memory of Dr Gustavo Torres-Cisneros.

Appendix

Proof of equation (24). We shall sketch the approximate evaluation of the integral over θ in $\tilde{C}$. The largest contribution to it comes from the factor $\exp[R_{\mathrm{cu}}(\beta_\alpha \Lambda_\alpha(\theta) + \beta_{\alpha'} \Lambda_{\alpha'}(\theta))]$, since R_{cu} is large. The following steps will be performed successively in $\tilde{C}$:

(a) we set $\theta = \pi/2$ in all factors, except in $\exp[R_{\mathrm{cu}}(\beta_\alpha \Lambda_\alpha(\theta) + \beta_{\alpha'} \Lambda_{\alpha'}(\theta))]$;
(b) we extend the integration over θ from $\theta = 0$ up to $\theta = \pi$;
(c) we evaluate the resulting integral by employing Laplace's method (see, for instance, Snyder and Love 1983). The fact that R_{cu} is large justifies these approximations. The result appears in equation (24).

Proof of equation (25). We consider an infinitesimal solid angle ω determined by the angles $\pi/2 - \theta_0 < \theta < \pi/2 + \theta_0$ and φ, $\varphi + \mathrm{d}\varphi$, $\mathrm{d}\varphi$ being small. Let σ be the intersection of ω and the spherical surface of large radius $|\vec{x}|$ ($\gg R_{\mathrm{cu}}$), the centre of which lies at $\vec{x} = (0, 0, 0)$ (see figure 3). Clearly, σ is a small (or infinitesimal) part of the finite surface Σ considered before, when evaluating F_{loss}. We consider the closed surface formed by σ and the surface $\sigma(\omega)$ which limits laterally the solid angle ω, as $|\vec{x}|$ varies from 0 up to the large radius which determines the intersection of ω with σ. In turn, $\sigma(\omega)$ is formed by the four lateral surfaces $\sigma(\omega; i)$, $i = 1, 2, 3, 4$, corresponding, respectively, to the constant values φ, $\theta = \pi/2 - \theta_0$, $\varphi + \mathrm{d}\varphi$ and $\theta = \pi/2 + \theta_0$. Notice that, for large R_{cu}, φ and $\varphi + \mathrm{d}\varphi$ correspond, approximately, to the transverse cross sections of the fibre at z and $z + \mathrm{d}z$,

respectively. Let $\langle F(z)\rangle$ be the probability flux of $\langle \vec{j}(\vec{x})\rangle$ across $\sigma(\omega; 1)$. Since the statistical average of the probability associated to the actual statistical mixture of wave functions is time-independent, $\langle \vec{j}(\vec{x})\rangle$ is conserved ($\vec{\nabla}\cdot\langle \vec{j}(\vec{x})\rangle = 0$). Then, total probability flux conservation applied to the closed surface formed by σ and $\sigma(\omega)$ yields:

$$\langle F(z+\mathrm{d}z)\rangle - \langle F(z)\rangle \simeq -\frac{\langle F_{\mathrm{loss}}\rangle}{R_{\mathrm{cu}}(\varphi_2-\varphi_1)}\mathrm{d}z = -\langle F_{\mathrm{in}}\rangle\tau_{\mathrm{av}}\mathrm{d}z. \tag{A.1}$$

Notice that $\langle F(z+\mathrm{d}z)\rangle$ and $\langle F(z)\rangle$ are, respectively, the probability fluxes across $\sigma(\omega; 3)$ and $\sigma(\omega; 1)$, while the fluxes across $\sigma(\omega; 2)$ and $\sigma(\omega; 4)$ have not been written in equation (A.1) (as they are negligible, by virtue of equation (16)). By using $\langle F(z_0)\rangle \simeq \langle F_{\mathrm{in}}\rangle$, and integrating equation (A.1) approximately for $z \geqslant z_0$, one gets equation (25).

An estimate of $B_\alpha(\pi/2)$. Let us turn to $B_\alpha(\pi/2)$ (equation (10)), with $\gamma_{1,\alpha}(\pi/2)$ replaced by the χ_α corresponding to the effectively propagating modes. Using the factor $\exp y'\chi_\alpha$, one estimates that the main contribution to $B_\alpha(\pi/2)$ comes from a region near $\boldsymbol{x}' = (x', d_{\mathrm{hcc}}/2)$, (as x' varies inside the allowed integration region in equation (10)). The size of that region appears to decrease as χ_α decreases towards χ_0, by virtue of the angular dependences of the propagation modes. A rather crude estimate would yield that $B_\alpha(\pi/2)$ is proportional to $\exp[2^{-1}\lambda_\alpha\chi_\alpha d_{\mathrm{hcc}}]$, $\lambda_\alpha < 1$. The magnitude of λ_α is largest for the fundamental mode and decreases as one proceeds to higher excited modes . This estimate appears to be roughly consistent with the results of some detailed related calculations in the two-dimensional case (see Calvo and Alvarez-Estrada 1986). Although the behaviour of τ_{av} for very large R_{cu} is not influenced by the factor $B_{\alpha'}(\pi/2)^{(*)}B_\alpha(\pi/2)$, the latter does play an increasing role in τ_{av} as R_{cu} decreases. The dominant contribution to $B_\alpha(\pi/2)\exp R_{\mathrm{cu}}\beta_\alpha\Lambda_\alpha(\pi/2)$ is roughly proportional to $q \equiv \exp\chi_\alpha[2^{-1}d_{\mathrm{hcc}}\lambda_\alpha - (1/3)[\chi_\alpha/\beta_\alpha]^2 R_{\mathrm{cu}}]$. Notice that, for given d_{hcc} and χ_α, the exponent of q changes sign, from positive to negative, when R_{cu} decreases below $R_{\mathrm{cu},0,\alpha} = (3\lambda_\alpha/2)(\beta_\alpha/\chi_\alpha)^2 d_{\mathrm{hcc}}$. The last equation is difficult to apply, in practice, in a precise way (as it would hold for any or most α characterizing an effectively propagating mode) but it seems to be some sort of analogue of the condition $R_{\mathrm{cu},0}\theta_{\mathrm{c}}^2(2d_{\mathrm{hcc}})^{-1} \simeq 1$, θ_{c} being the critical angle, derived in the framework of geometrical optics (see equation (23) in Kumakhov and Komarov 1990). The above discussion suggests that there is some $R_{\mathrm{cu}} = R_{\mathrm{cu},0}$ ($R_{\mathrm{cu},0}$ being some sort of average of the $R_{\mathrm{cu},0,\alpha}$, as α runs over the effectively excited modes) such that, for $R_{\mathrm{cu}} < R_{\mathrm{cu},0}$, $\exp[R_{\mathrm{cu}}(\beta_\alpha\Lambda_\alpha(\pi/2) + \beta_{\alpha'}\Lambda_{\alpha'}(\pi/2))]$ is overcome by $B_{\alpha'}(\pi/2)^{(*)}B_\alpha(\pi/2)$.

References

Alvarez-Estrada R F and Calvo M L 1984 *J. Phys. D: Appl. Phys.* **17** 475

Bacon G E 1962 *Neutron Diffraction* (Oxford: Clarendon)

Berry M V and Mount K E 1972 *Rep. Prog. Phys.* **35** 315

Born M and Wolf E 1999 *Principles of Optics* 7 edn, ch X (Cambridge: Cambridge University Press)

Calvo M L and Alvarez-Estrada R F 1986 *J. Phys. D: Appl. Phys.* **19** 957

——1987 *J. Opt. Soc. Am.* A **4** 683

Chen H, Downing R G, Mildner D F R, Gibson W M, Kumakhov M A, Ponomarev I Yu and Gubarev M V 1992 *Nature* **357** 391

Glauber R J 1959 *Lectures in Theoretical Physics* vol 1 (New York: InterScience)

Jacrot B 1970 *Proc. Symp. Instrumentation for Neutron Inelastic Scattering Research (Vienna 1969)* (Vienna: IAEA)

Kumakhov M A and Komarov F F 1990 *Phys. Rep.* **191** 289

Kumakhov M A and Sharov V A 1992 *Nature* **357** 390

Marcatili E A J 1969 *Bell Syst. Tech. J.* **48** 2103

Marcuse D 1972 *Light Transmission Optics* (New York: Van Nostrand-Reinhold)

——1974 *Theory of Dielectric Optical Waveguides* (New York: Academic)

——1976 *J. Opt. Soc. Am.* **66** 216

Martin A 1972 *Helv. Phys. Acta* **45** 140

Messiah A 1961 *Quantum Mechanics* vol I (Amsterdam: North-Holland)

Schaerpf O and Eichler D 1973 *J. Phys. E: Sci. Instrum.* **6** 774

Sears V F 1989 *Neutron Optics* (New York: Oxford University Press)

Snyder A W and Love J D 1983 *Optical Waveguide Theory* ch 23 (London: Chapman and Hall)